Comparative modeling of pivotal enzymes, MurA and MurZ, of Enterococcus faecalis and identification of potential inhibitors by computational methods

ARTICLE *in* MEDICINAL CHEMISTRY RESEARCH · SEPTEMBER 2013

Impact Factor: 1.4 · DOI: 10.1007/s00044-013-0785-z

Med Chem Res
DOI 10.1007/s00044-013-0785-z

MEDICINAL CHEMISTRY RESEARCH

ORIGINAL RESEARCH

Comparative modeling of pivotal enzymes, MurA and MurZ, of *Enterococcus faecalis* and identification of potential inhibitors by computational methods

Mansimran Khokhar · Navkiran Kaur · Vaibhav Jain · Rajat Sandhir · Ankur Gautam · Prasad V. Bharatam · Rupinder Tewari

Received: 9 January 2013 / Accepted: 10 September 2013

Abstract The emergence of multi-drug-resistant bacterial pathogens along with labor-intensive and time-consuming drug discovery methods has put an emphasis on alternative approaches which can overcome these drawbacks. One such approach is in silico identification of novel bacterial inhibitors using structure-based drug design methodology. In the present study, novel inhibitors have been proposed against two essential enzymes (MurA and MurZ) involved in the biosynthesis of cell wall of *Enterococcus faecalis*, a serious nosocomial bacterial pathogen. Homology models of MurA and MurZ of *E. faecalis* were constructed using template MurA of *Enterobacter cloacae* and *Haemophilus influenza*, respectively. The validation of the refined models, using Ramachandran, Errat and ProSA energy plots, showed that constructed models were reliable and of good quality. The active site amino acid residues, as predicted by CASTp server, were in accordance with the residues identified from MurA crystal structures available for other bacteria. The present study revealed for the first time the importance of two additional amino acid residues (Thr305 and Tyr329) in MurA and MurZ enzymes, which might be crucial for the binding of ligands/inhibitors with the target. Based on the GLIDE score and interaction profile, 5-sulfonoxy-anthranilic acid derivatives, T6361 and T6362 were found to be the potential inhibitors of MurA and MurZ enzymes.

Keywords *Enterococcus faecalis* · Peptidoglycan · MurA · MurZ · Homology modeling · Molecular docking

M. Khokhar · N. Kaur · A. Gautam · R. Tewari (✉)
Centre for Microbial Biotechnology, Panjab University, CIL Building, Chandigarh, India
e-mail: rupinder@pu.ac.in

V. Jain · P. V. Bharatam
Department of Pharmacoinformatics, National Institute of Pharmaceutical Education and Research (NIPER), Mohali, India

R. Sandhir
Department of Biochemistry, Panjab University, Chandigarh, India

Introduction

Enterococcus faecalis (*E. faecalis*) is a bacterial pathogen, which has gained notoriety over the past few decades as the leading cause of nosocomial infections causing urinary tract problems, bacteremia, intra-abdominal infections and endocarditis with a high mortality rate (Bao *et al.*, 2009; Sav *et al.*, 2010). Though antibiotic therapy is available for treatments of this infection, drug-resistant clinical isolates of *E. faecalis* are being regularly isolated from laboratories all over the world (Sood *et al.*, 2008). This grim situation along with the fact that limited research is being carried out to screen novel *Enterococci* inhibitors' demands for an urgent need for new drug targets and specific inhibitors. The availability of the gene and protein sequences of pathogens, including *E. faecalis,* has brought forth extensive information that can be useful for novel drug target identification and drug development (Meinke *et al.*, 2004).

A peptidoglycan (PG) layer is an integral component of bacterial cell wall. The absence of PG has been shown beyond doubt to cause cell death (Babajan *et al.*, 2011). The essentiality of PG layer along with its absence in eukaryotic cells has resulted in exploiting the enzymes of PG biosynthesis as potential drug targets. The initial steps in PG biosynthesis are mediated by a group of Mur enzymes (Samland *et al.*, 2001; Klein and Bachelier, 2006). As Mur enzymes are absent in humans and have no human homologs, they represent a promising point of

Published online: 19 September 2013

attack for novel antibacterial drugs. In Gram-positive bacteria including *E. faecalis*, *murA* gene has two copies (*murA* and *murZ*) which encode proteins with similar enzymatic activity. Studies have also brought forth the fact that removal of both the genes is necessary for cell wall disruption in *E. faecalis* (Du *et al.*, 2000). Although, structure of MurA enzymes from Gram-negative bacteria has been deciphered and inhibitors reported (Dunsmore *et al.*, 2008; Eschenburg *et al.*, 2005), but none from Gram-positive bacteria has been reported. In this article, attempt has been made to develop homology models for $MurA_{ef}$ and $MurZ_{ef}$ enzymes of *E. faecalis* and novel inhibitors against these targets have been identified.

Materials and methods

Homology modeling of $MurA_{ef}$ and $MurZ_{ef}$

The protein sequences of $MurA_{ef}$ and $MurZ_{ef}$ were retrieved from UNIPROT database (http://www.uniprot.org/). To find a suitable template for model building, NCBI BLASTp (Altschul *et al.*, 1990) was performed against Protein Data Bank (PDB). ClustalW (http://www.ebi.ac.uk/Tools/msa/clustalw2) tool was used to carry out protein multiple sequence alignments. The three dimensional (3D) model of the enzymes along with the ligand present in the template was built using Modeller9v8 (http://www.salilab.org/modeller/). Subsequently, model validation was carried out using PROCHECK (Laskowski *et al.*, 1993) and ProSA-web (Sippl, 1993) programs. PROCHECK scrutinizes the stereochemical quality of a protein structure and presents a Ramachandran plot of the query structure. Steric clashes observed in the crude models were recognized by the ERRAT plot and the structural loops showing error greater than 90 % were refined through loop modeling using Modeller Loop class (Colovos and Yeates, 1993). PDBsum server was used to analyze the secondary structure of the proteins (Laskowski *et al.*, 2009). The active site prediction of the modeled enzymes was performed using the computed atlas of surface topography of proteins (CASTp) server. It provides identification and measurements of surface accessible pockets as well as interior inaccessible cavities for proteins by analytically measuring the area and volume of each pocket and cavity, both in solvent accessible surface and molecular surface (Kaistha and Sinha, 2009).

Molecular docking

Retrieval of ligands and database generation

The literature sources were surveyed for small inhibitory compounds and a total of 108 compounds were retrieved. These compounds were chosen on their reports of inhibiting MurA from various microorganisms e.g., *Staphylococcus aureus*, *Mycobacterium tuberculosis*, *E. cloacae*, *H. influenza*, and *Bacillus anthracis*. The 3D structures of these ligands were built using SYBYL 7.1 molecular modeling package installed on a Silicon Graphics Fuel Workstation (Baviskar *et al.*, 2011). Gasteiger-Hückel partial charges were applied to the atoms of the ligand followed by minimization of the structures by Powell method using Tripos force field. Finally, 3D database of ligands was generated in SYBYL.

Ligand and enzyme structure preparation

The LigPrep module of Maestro (Maestro 9.0, Schrödinger, LLC, New York) interface was used for the preparation of ligand structures from the generated database. It optimizes each ligand structure to produce low energy, tautomeric, and reasonable ionization state conformations within a range of pH 7.0 $\pm$ 2.0 using OPLS_2005 force field.

The refined and validated structures of $MurA_{ef}$ and $MurZ_{ef}$ enzymes were processed using Protein Preparation wizard tool incorporated in Maestro interface. Hydrogen atoms were added and the right bond orders were assigned to the enzymes. The carboxylic acid side chains of all the Asp and Glu residues were deprotonated and basic residues Lys and Arg side chains were protonated so as to mimic correct ionization state at physiological pH. In addition, correct tautomeric state of His and the spatial arrangements of hydroxyl and amide groups of Asn and Gln were defined using Protassign utility (Schrödinger Suite, 2009). To remove the steric clashes between the atoms, enzyme structures were minimized using Impref utility until the average root-mean-square-deviation (RMSD) of the complete atoms came down to 0.3 Å.

Receptor grid generation

Receptor grid generation module of GLIDE was used to define the receptor grid. The ligands UNAG and UD1 (bound to $MurA_{ef}$ and $MurZ_{ef}$) were taken as reference to designate the active site of $MurA_{ef}$ and $MurZ_{ef}$, respectively. The centroid of the bound ligand was used to define the inner box of the grid by extending the dimension to 10 Å and the external box by extending up to 20 Å. This step determines the position and size of the active site of the target, thus setting up Glide constraints (Schrödinger Suite, 2009). These constraints were then used to fit/dock ligands into the target site.

Molecular docking

Docking simulations were performed using Grid-based Ligand Docking with Energetics (GLIDE) program. Glide

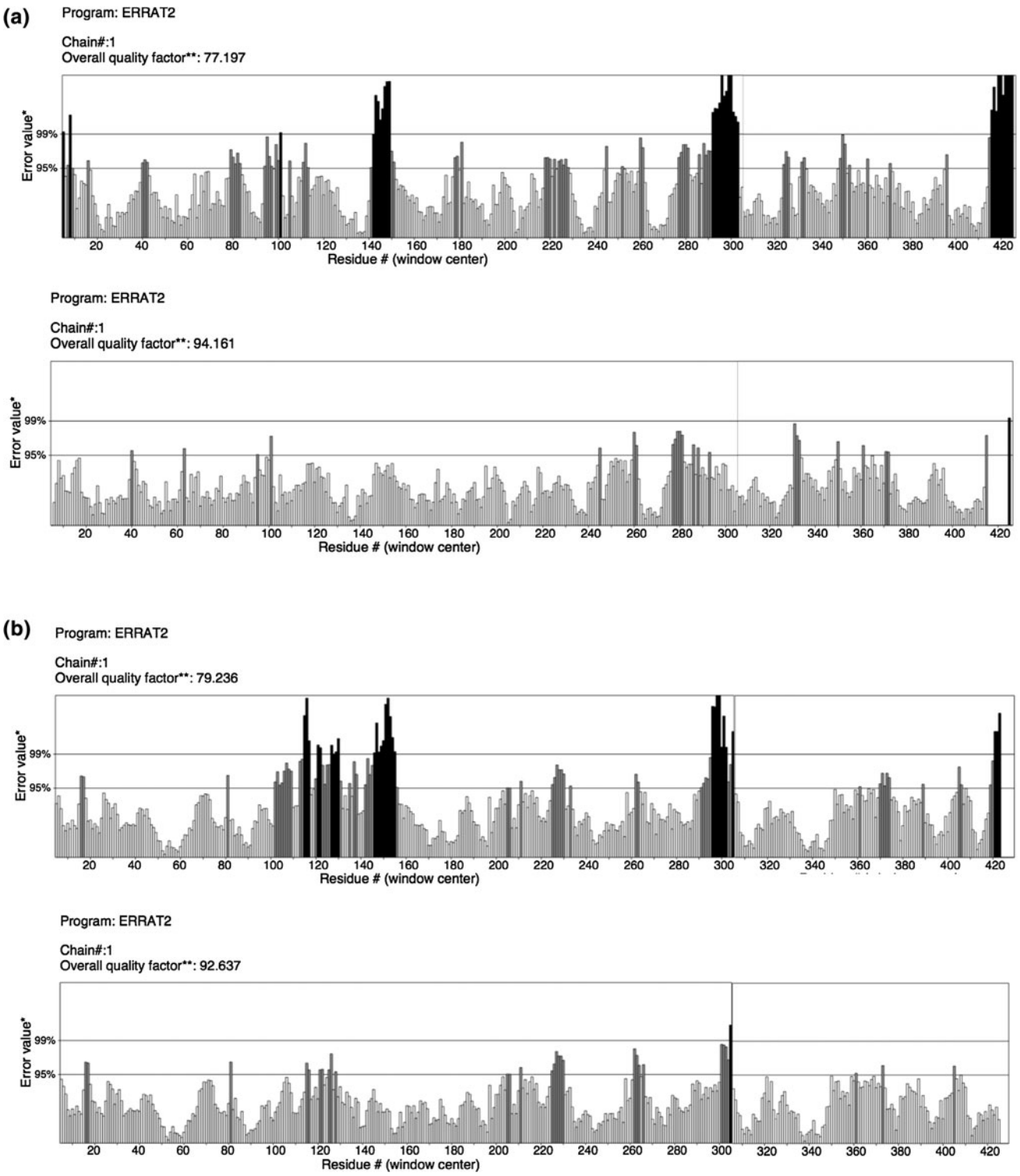

Fig. 1 ERRAT plot of **(a)** $MurA_{ef}$ and **(b)** $MurZ_{ef}$ enzymes

explores for possible locations of the ligand in the active site region of the enzymes using a set of hierarchal filters. It searches for favorable interactions between one or more conformations of the ligands and a protein (Friesner *et al.*, 2004). The ligand is minimized in the field of the receptor using the OPLS-AA force field. The ChemScore algorithm was used to perform scoring, recognizing favorable hydrophobic and hydrogen bond interactions (Eldridge *et al.*, 1997).

Results and discussion

Template selection

The 430 amino acids long protein sequence of $MurA_{ef}$ was retrieved from UNIPROT/SwissProtKB database (primary accession number: Q836E5). After performing BLASTP analysis against PDB database, maximum sequence homology was found with MurA from *E. cloacae* (PDB ID: 1Q3G, Ligand: UDA (3′-1-carboxy-1-phosphonooxy-ethoxy-uridine-diphosphate-*N*-acetylglucosamine), Resolution: 2.65 Å) (Eschenburg *et al.*, 2003). It exhibited 46 % sequence identity and an E value of $7e^{-121}$. Correspondingly, the template search for $MurZ_{ef}$ (primary accession number: Q831A8) demonstrated maximum sequence homology with MurA from *H. influenza* [PDB ID: 2RL1, Ligand: UD1 (uridine-diphosphate-*N*-acetylglucosamine), resolution: 2.20 Å] (Yoon *et al.*, 2008). It exhibited 48 % identity with an E value of $3e^{-131}$. Owing to the fact that both $MurA_{ec}$ (1Q3G) and $MurA_{hi}$ (2RL1) exhibited high sequence identity and the PDB's had bound ligands in their crystal structures, made them suitable for being used as templates. This allowed us to model the ligand within our homology models. In addition, the resolution of both of these crystal structures was high (1Q3G: 2.65 Å and 2RL1: 2.20 Å), and they posses overall good B-factor, therefore, they were used as templates for homology modeling for $MurA_{ef}$ and $MurZ_{ef}$ proteins, respectively.

Homology modeling

Based on the information obtained from the sequence alignment of target ($MurA_{ef}$) and template (1Q3G) protein sequence, the homology model of $MurA_{ef}$ was generated by Modeller9v8. 100 models were generated and the model with lowest discrete optimized protein energy (DOPE) and Molpdf scores was selected for further optimization. Steric clashes were observed in the loop regions of the crude model, therefore, these regions were further subjected to loop

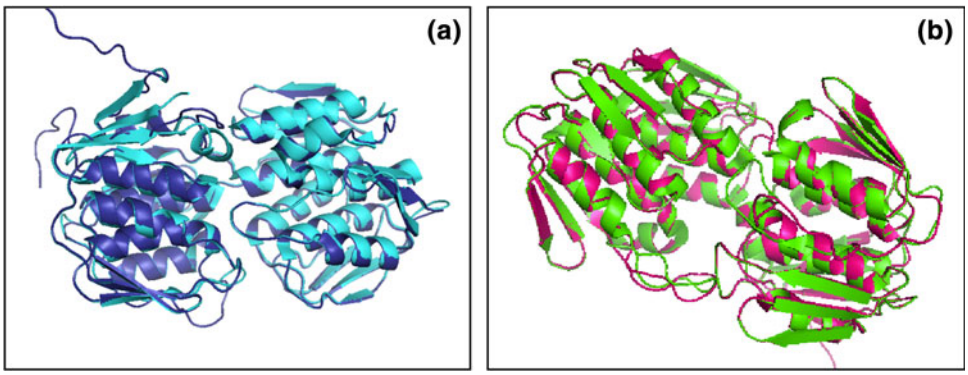

Fig. 2 Superimposition of **(a)** $MurA_{ef}$ (*cyan*) homology model with template 1Q3G (*blue*) and **(b)** $MurZ_{ef}$ (*green*) homology model with template 2RL1 (*magenta*) (Color figure online)

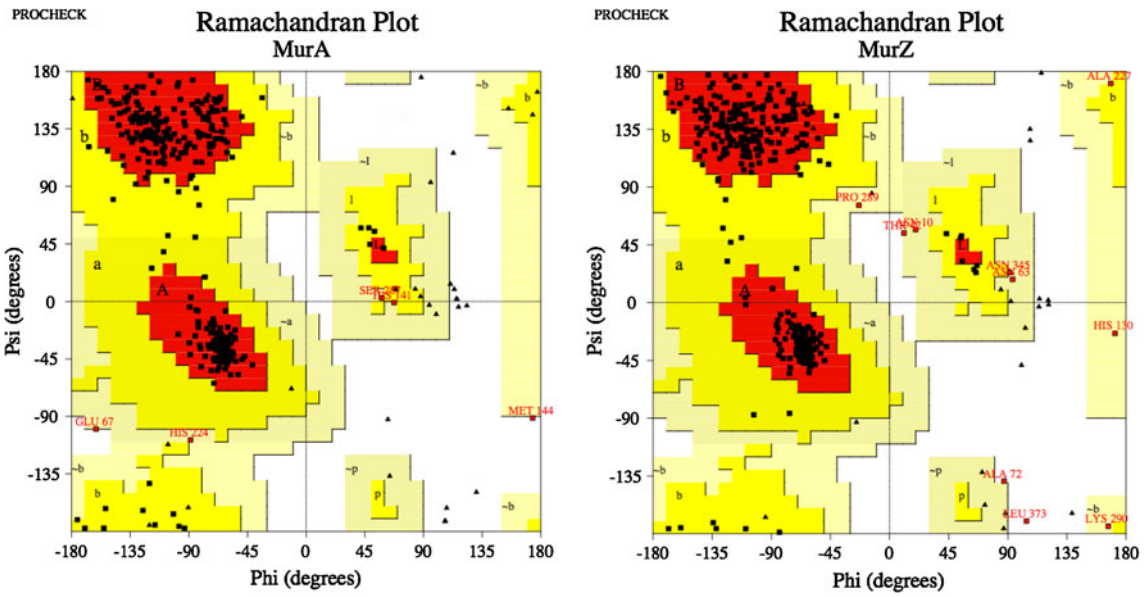

Fig. 3 Ramachandran plots of $MurA_{ef}$ and $MurZ_{ef}$ enzymes

modeling using Modeller Loop class. The model of $MurA_{ef}$ also contained the modeled ligand: UDP-*N*-acetylglucosamine (UNAG) (substrate). Similarly, homology model of $MurZ_{ef}$ was generated using 2RL1 as the template structure and contained the modeled ligand: UDP-*N*-acetylglucosamine, referred to as UD1 (substrate). After a few cycles of loop refinement, the 3D models of MurA and MurZ exhibited an overall quality factor of 94.16 and 92.64 %, respectively (Fig. 1).

The superimposition of Cα chains of 1Q3G and $MurA_{ef}$ (Fig. 2a) revealed an RMSD value of 0.421 Å. Also RMSD value of 0.199 Å was observed when 2RL1 and $MurZ_{ef}$ (Fig. 2b) were superimposed. The RSMD values were in acceptable range i.e., ≤0.5 Å, suggesting the validity of the models constructed.

Evaluation of homology models of MurA and MurZ enzymes

Validation tools like PROCHECK, VERIFY3D, and ERRAT were used for protein structure evaluation. The $MurA_{ef}$ Ramachandran plot, generated by PROCHECK (Fig. 3), revealed that 89 % residues were in the most favored region, 9.3 % in the additionally allowed region, 1.1 % in the generously allowed region and 0.5 % in the disallowed region, thereby indicating that $MurA_{ef}$ model was geometrically acceptable. For $MurZ_{ef}$, the Ramachandran plot demonstrated that 89.8 % residues were in the most favored region, 7.9 % in the additionally allowed region, 1.8 % in the generously allowed region and 0.5 % in the disallowed region (Fig. 3). This data suggested the

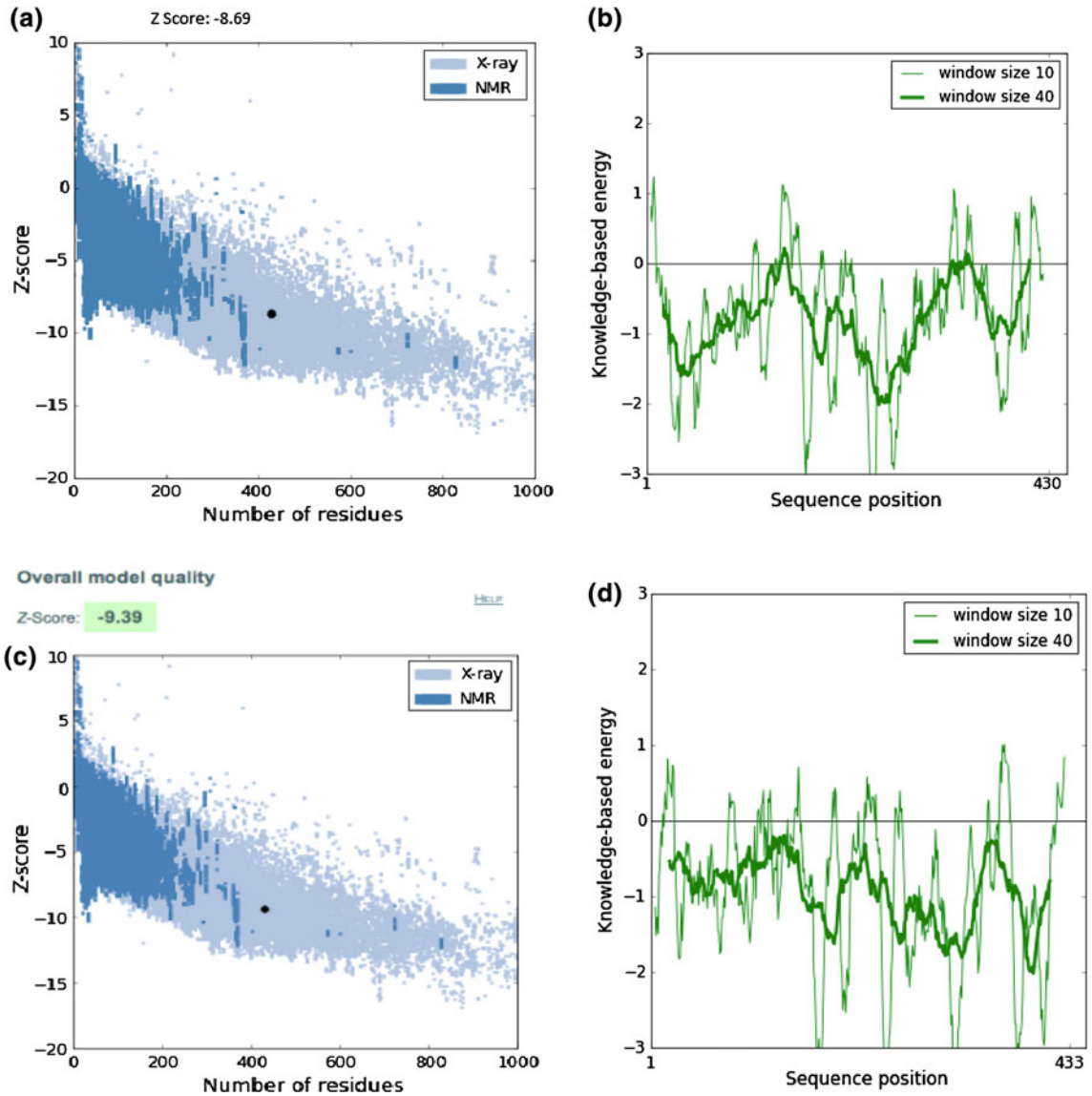

Fig. 4 *Z*-score and residue energy plots of **(a)**, **(b)** $MurA_{ef}$ and **(c)**, **(d)** $MurZ_{ef}$ enzymes

geometrical and stereochemical acceptability of the model. As the residues in the disallowed regions did not show any involvement in the active site/ligand binding, they were left as such and the model was not further modified.

The reliability and accuracy of the developed models was further evaluated by generating knowledge-based energy curves for $MurA_{ef}$ and $MurZ_{ef}$ using ProSA-web (Fig. 4) (Wiederstein and Sippl, 2007). The *z*-score calculated by ProSA indicated the overall quality of the models. The *z*-score of $MurA_{ef}$ (Fig. 4a) and $MurZ_{ef}$ (Fig. 4c) was observed to be well within the *z*-score range of experimentally determined NMR solved protein structures. The plots (Fig. 4b, d) of residue energy exhibit the local model quality by plotting energies as a function of amino acid sequence position with different window size. Also, the ProSA-web application requires only C-α backbone; therefore, it allows us to evaluate the models early in structure determination process. These energy plots describe the problematic parts of the model corresponding to the positive values. In our model, most of the amino acid sequences exhibit negative knowledge-based energy, signifying that the overall quality of the model is satisfactory.

Secondary structure analysis

The secondary structure of $MurA_{ef}$ was analyzed using PDBsum server, which showed that it consisted of 17 helices, 6 beta sheets, 20 strands, 5 beta hairpins, 1 beta bulge, 2 beta–alpha–beta motifs, 31 helix–helix interactions, 23 beta turns, and 4 gamma turns (Fig. 5a) (Dundas *et al.*, 2006). Similarly, the secondary structure of $MurZ_{ef}$ depicted 19 helices, 6 beta sheets, 22 strands, 5 beta hairpins, 2 beta bulges, 2 beta-alpha–beta motifs, 29 helix–helix interactions, and 22 beta turns (Fig. 5b) (Dundas *et al.*, 2006). As structure and function of the protein are inter-correlated, this analysis provides detailed insight into the structure of the MurA/MurZ enzymes, which could be used to determine their function by comparing the topology with existing 3D structures of Mur enzymes of different organisms.

Active site prediction

Active site prediction, of constructed enzyme models, using CASTp server suggested different binding pockets. Based on the volume and area of the cavities and pocket, ranking was assigned to the predictive active site. Rank 1 predicted active site cavity in $MurA_{ef}$ and $MurZ_{ef}$ enzymes composed of 70 and 74 amino acid residues, respectively. These showed the presence of Lys22, Asn23, Asp49, Arg92, Cys116, Arg121, and Arg398 in the active site of $MurA_{ef}$ (Fig. 6a). The amino acid residues predicted were

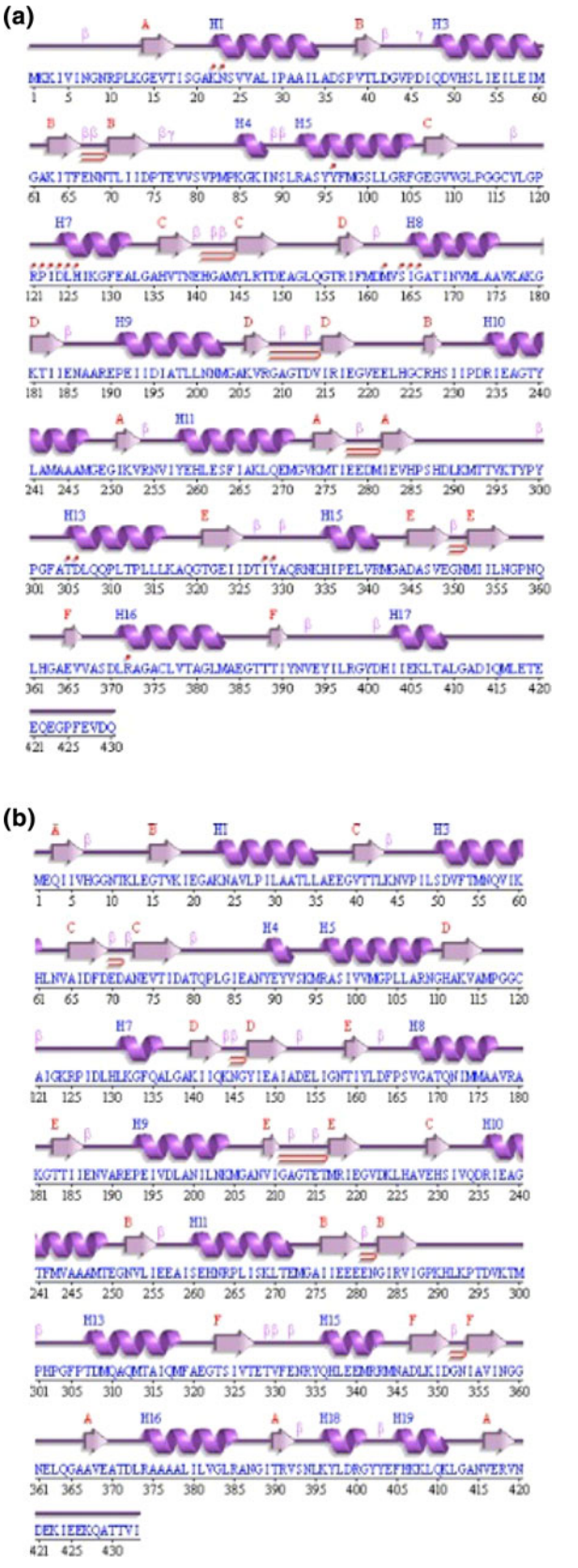

Fig. 5 Diagrammatic representation of secondary structural elements of **(a)** $MurA_{ef}$ and **(b)** $MurZ_{ef}$ enzymes

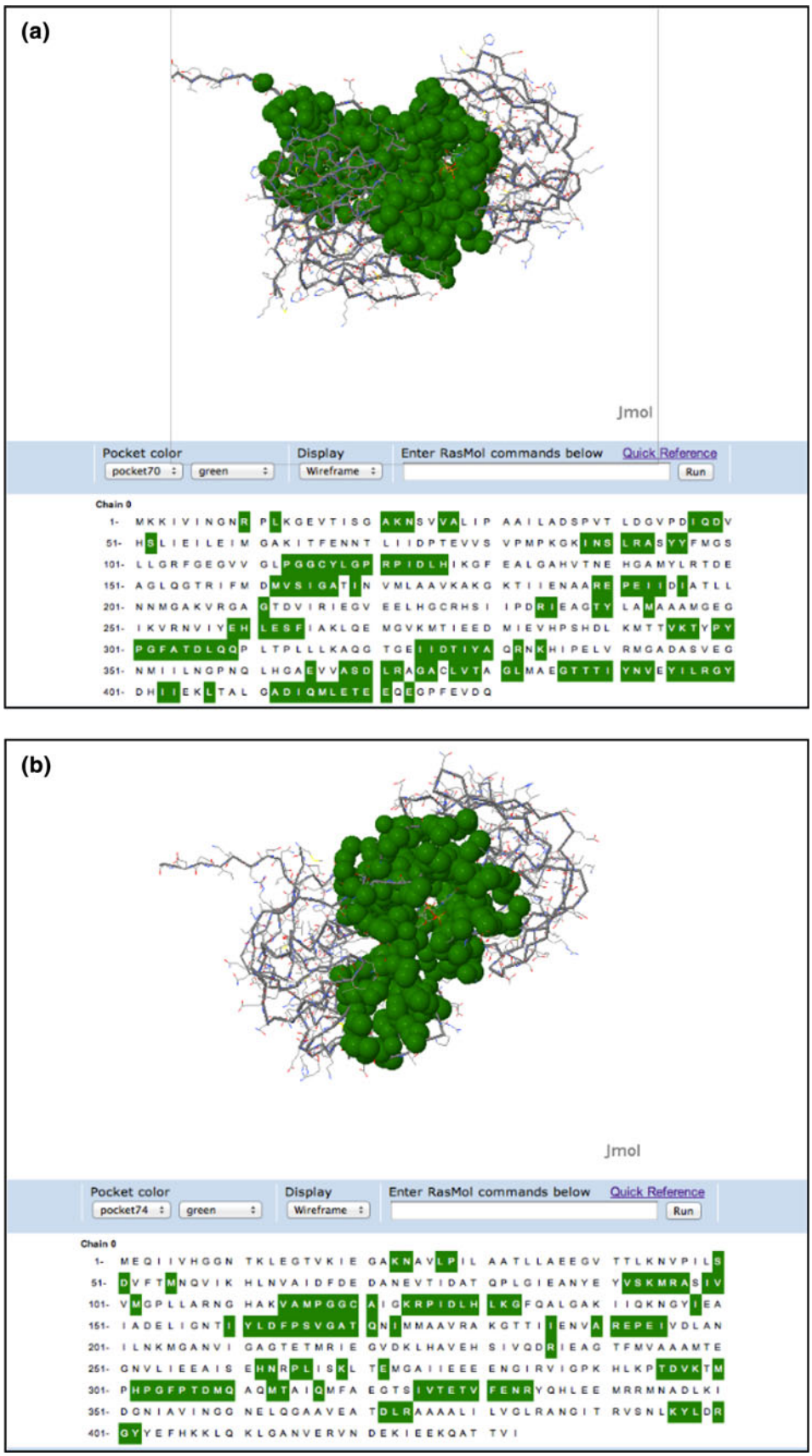

Fig. 6 CASTp analysis of **(a)** $MurA_{ef}$ and **(b)** $MurZ_{ef}$ enzymes. The predicted binding site is highlighted in *green* (Color figure online)

Table 1 Docking score and hydrogen bonding interactions of ligands with MurA and MurZ enzymes

Ligand	Structure	GLIDE docking score		Hydrogen bonding interactions	
		MurA	MurZ	MurA	MurZ
T6361	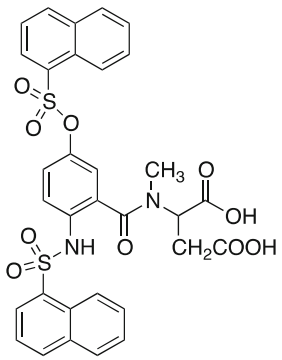	−7.466	−7.984 (Fig. 7b)	**Arg92**, **Arg121**, **Pro122**, **His 126**, **Ile165**, **Gly166**	**Lys23**, **Arg96**, **Arg125**, **His130**, **Ser166**, **Gly168**, **Thr307**
T6362	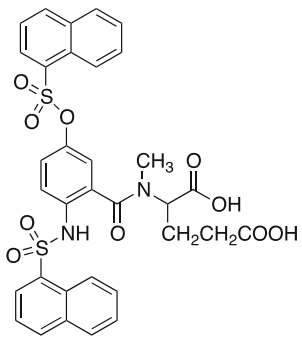	−8.252 (Fig. 7a)	−7.439	**Arg121**, **His126**, **Ile165**, **Gly166,** Ala167, Thr305, Tyr329	**Arg96**, **Arg125**, **Val167**, **Arg400**
Carbidopa	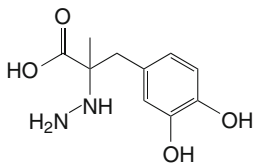	−5.665	−6.789	**Asp49**, **Arg121**, **Arg332**, Thr 305, Tyr329	**Lys23**, **Asn24**, **Arg125**, **Gln171**, **Asp308**

Residues in bold represent the amino acids reported to be essential for enzymatic activity [8, 11, 27, 28, 29, 30, 32]. These interactions were in accordance with the ones shown by available crystal structures of MurA enzymes from different organisms

also found to be present in the active site of the template structure (1Q3G) and have been reported to be imperative for other bacteria as well (Jackson *et al.*, 2009; Kim *et al.*, 1996; Skarzynski *et al.*, 1996). Similarly, Lys23, Arg96, Cys120 Arg125, Asp308, and Arg400 were found to be present in the active sites of $MurZ_{ef}$, template 2RL1 (Fig. 6b) and other bacteria as well (Gautam *et al.*, 2011; Schonbrunn *et al.*, 2000).

Virtual screening employs computational methods for the identification of molecules that may be biologically active against a target protein. We have adopted Structure-based virtual screening, for the identification of novel inhibitors against the target protein(s) MurA and MurZ of *E. faecalis*. A small library of compounds was built for the purpose of performing molecular docking. Due to the absence of 3D structure of target proteins, we developed homology models of the same. These models were generated using Modeller, which were then subjected to loop refinement and optimization. The final refined homology models showed satisfactory Ramachandran plot statistics, Errat plot quality factor. Moreover, the online validation server (ProSA web) showed that the Z-score and energy of protein folding of the models was in good agreement with the available protein structures in PDB, which favored the overall quality of the structures. These analyses validated the homology models and prove that they are robust as well as reliable enough to be used for virtual screening purpose.

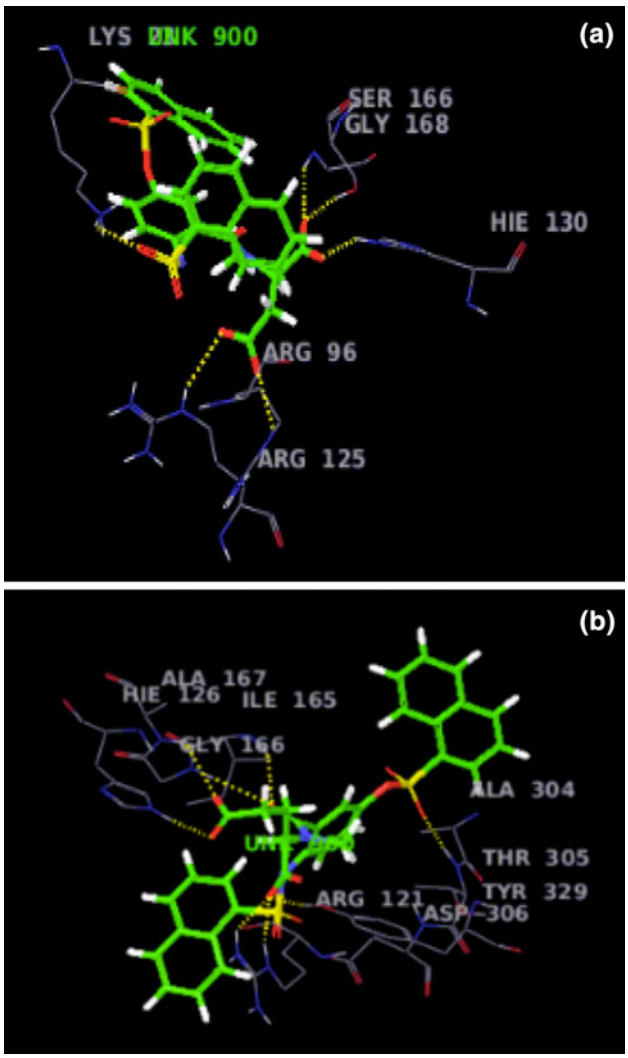

Fig. 7 Interaction profile of **(a) T6362** with $MurA_{ef}$ and of **(b) T6361** with $MurZ_{ef}$ (the *yellow dashed lines* mark the hydrogen bonding interactions) (Color figure online)

Molecular docking analysis

In order to study the molecular level interactions and binding affinity of the reported inhibitors (active for Mur of other organisms) against $MurA_{ef}$ and $MurZ_{ef}$, they were subjected to molecular docking into the active site of enzyme structures using GLIDE (Table 1) program. For selecting the ligands as probable inhibitor of $MurA_{ef}$ and $MurZ_{ef}$, a limit of Glide score (<-5.00) and hydrogen bonding interactions (≥ 3) with the critical amino acid residues of the active site was set. Based on the minimal energy binding score, an indicative of good docking, ligands **T6362** and **T6361** were found to be the best possible inhibitors of $MurA_{ef}$ and $MurZ_{ef}$ respectively. Both these inhibitors are derivatives of 5-sulfonoxy-anthranilic acid. Previous studies reveal the action of **T6361** as a competitive inhibitor of the substrate (UNAG). It targets a loop from Pro112 to Pro125 (which induces a conformational change in the enzyme), thus preventing the access of UNAG to the active site. Binding mode of T6362 (Fig. 7a) revealed hydrogen bonding with main chain atoms of **Arg92**, **Gly166**, **and Thr305** and with side chain atoms of Arg121, His126, Ile165, Ala167, and Tyr329. It also showed π-interactions with **Tyr95** and **His126**. The binding mode of T6361 (Fig. 7b) revealed hydrogen bonding with main chain atoms of **Lys23**, **Arg96**, **and Gly168** and with side chains Arg125, His130, Ser166, and Thr307. It also showed π-interactions with **Phe331**. These interactions were in accordance with the ones shown by available crystal structures of MurA enzymes from different organisms. **Carbidopa** which has been identified as a promiscuous inhibitor, and reported to inhibit even MurA C115D mutant also showed a good docking profile. These compounds have previously been reported to inhibit MurA of different organisms thereby advocating their broad host range (BHR) activity (Dunsmore *et al.*, 2008; Laskowski *et al.*, 1993). GLIDE evidence also suggested two residues (Thr305/307 and Tyr329), which might be noteworthy but have not been reported previously. The inference can be drawn out of the fact that, the interactions shown by these residues have been repeated while studying docking with different ligands. In the absence of any known ligands for $MurA_{ef}$ and $MurZ_{ef}$, these inhibitors could act as leads and thus can be used as starting point for designing other inhibitors as well.

Conclusions

Using in silico structure-based drug designing approach, computational models of enzymes (MurA and MurZ) of a serious nosocomial bacterium, *E. faecalis* have been developed. Molecular docking procedure has resolved to three molecules namely T6361, T6362, and Carbidopa, which can act as potential anti-microbial agents. A report of these compounds also inhibiting MurA of different organisms advocates their BHR activity.

References

Altschul SF, Grish W, Miller W, Myers EW, Lipman DJ (1990) Basic local alignment search tool. J Mol Biol 215:403–410

Babajan B, Chaitanya M, Rajsekhari C, Gowsia D, Madhusudhana P, Naveen M, Chittai SK, Anuradha CM (2011) Comprehensive structural and functional characterization of *Mycobacterium tuberculosis* UDP-NAG enolpyruvyl transferase (Mtb–MurA) and prediction of its accurate binding affinities with inhibitors. Interdiscip Sci Comput Life Sci 3:204–216

Bao Y, Saknic T, Laverde D, Wobser D, Benachour A, Theilacker C, Hartke A, Huebner J (2009) Role of *mprF1* and *mprF2* in the pathogenicity of *Enterococcus faecalis*. PLoS One 7:38458

Baviskar AT, Madaan C, Preet R, Mohapatra P, Jain V, Agrawal A, Guchhait SK, Kundu CN, Banerjee CN, Bharatam PV (2011) N-Fused imidazoles as novel anticancer agents that inhibit catalytic activity of topoisomerase IIα and induce apoptosis in G1/S Phase. J Med Chem 54:5013–5030

Colovos C, Yeates TO (1993) Verification of protein structures: patterns of nonbonded atomic interactions. Protein Sci 9:1511–1519

Du W, Brown JR, Sylvester DR, Huang J, Chalker AF, So CY, Holmes DJ, Payne DJ, Wallis NJ (2000) Two active forms of UDP-*N*-acetylglucosamine enolpyruvyl transferase in gram-positive bacteria. J Bacteriol 182:4146–4152

Dundas J, Ouyang Z, Tseng J, Binkowski A, Turpaz Y, Liang J (2006) CASTp: computed atlas of surface topography of proteins with structural and topographical mapping of functionally annotated residues. Nucleic Acid Res 34:W116–W118

Dunsmore CJ, Miller K, Blake KL, Patching SG, Henderson PJF, Gaenett JA, Stubbings WJ, Phillips SVE, Palestrant DJ, Angeles JDL, Leeds JA, Choprab I, Fishwicka CWG (2008) 2-Aminotetralones: novel inhibitors of MurA and MurZ. Bioorg Med Chem Lett 18:1730–1734

Eldridge MD, Murray CW, Auton TR, Paolini GV, Mee RP (1997) Empirical scoring functions: I. The development of a fast empirical scoring function to estimate the binding affinity of ligands in receptor complexes. J Comput Aided Mol Des 11:425–445

Eschenburg S, Kabsch W, Healy ML, Schoenbrunn E (2003) A new view of the mechanism of UDP-*N*-acetylglucosamine enolpyruvyl transferase (MurA) and 5-enolpyruvylshikimate-3-phosphate synthase (AroA) derived from X-ray structures of their tetrahedral reaction intermediate states. J Biol Chem 278:49215–49222

Eschenburg S, Priestman M, Schonbrunn E (2005) Evidence that the fosfomycin target Cys115 in UDP-*N*-acetylglucosamine enolpyruvyl transferase (MurA) is essential for product release. J Biol Chem 280:3757–3763

Friesner RA, Banks JL, Murphy RB, Halgren TA, Klicic JJ, Mainz DT, Repasky MP, Knoll EH, Shelley M, Perry JK, Shaw DE, Francis P, Shenkin PS (2004) Glide: a new approach for rapid, accurate docking and scoring. 1. Method and assessment of docking accuracy. J Med Chem 47:1739–1749

Gautam A, Rishi P, Tewari R (2011) UDP-*N*-acetylglucosamine enolpyruvyl transferase as a potential target for antibacterial chemotherapy: recent developments. Appl Microbiol Biotechnol 92:211–225

Jackson SG, Zhang F, Chindemi P, Junop MS, Berti PJ (2009) Evidence of kinetic control of ligand binding and staged product release in MurA (Enolpyruvyl UDP-GlcNAc synthase)-catalyzed reactions. Biochemistry 48:11715–11723

Kaistha SD, Sinha R (2009) Homology modeling of phosphoryl thymidine kinase of enterohemorrhagic *Escherichia coli* OH: 157. Bioinformation 6:240–243

Kim DH, Lees WJ, Kempsell KE, Lane WS, Duncan K, Walsh CT (1996) Characterization of a Cys115 to Asp substitution in the *Escherichia coli* cell wall biosynthetic enzyme UDP-GlcNAcenolpyruvyl transferase (MurA) that confers resistance to inactivation by the antibiotic fofomycin. Biochemistry 35:4923–4928

Klein CD, Bachelier A (2006) Molecular modeling and bioinformatical analysis of the antibacterial target enzyme MurA from a drug design perspective. J Comput Aided Mol Des 20:621–628

Laskowski RA, MacArthur MW, Moss DS, Thornton JM (1993) PROCHECK: a program to check the stereochemical quality of protein structures. J Appl Crystallogr 26:283–291

Laskowski RA, Chistyakov VV, Thornton JM (2009) PDBSUM more: new summaries and analyses of the known 3-D structures proteins and nucleic acids. Nucleic Acid Res 33:266–268

Meinke A, Henics T, Nagy E (2004) Bacterial genomes pave the way to novel vaccines. Curr Opin Microbiol 7:314–320

Samland AK, Esfarjani TE, Amrhein N, Macheroux P (2001) Asparagine 23 and Aspartate 305 are essential residues in the active site of UDP-*N*-acetylglucosamine enolpyruvyl transferase from *Enterobacter cloacae*. Biochemistry 40:1550–1559

Sav IG, Heikens E, Huebner J (2010) Pathogenesis and immunity in enterococcal infections. Clin Microbiol Infect 16:533–540

Schonbrunn E, Eschenburg S, Krekel F, Luger K, Amrhein N (2000) Role of the loop containing residue 115 in the induced-fit mechanism of the bacterial cell wall biosynthetic enzyme MurA. Biochemistry 39:2164–2173

Schrödinger Suite (2009) Protein preparation wizard; Epik version 2.0, Schrödinger, LLC, New York, NY, 2009; Impact version 5.5, Schrödinger, LLC, New York, NY, 2009; Prime version 2.1, Schrödinger, LLC, New York, NY, 2009

Sippl MJ (1993) Recognition of errors in three-dimensional structures in proteins. Proteins 17:355–362

Skarzynski T, Mistry A, Wonacott A, Hutchinson SE, Kelly VA, Duncan K (1996) Structure of UDP-*N*-acetylglucosamine enolpyruvyl transferase, an enzyme essential for the synthesis of bacterial peptidoglycan, complexed with substrate UDP-*N*-acetylglucosamine and the drug fosfomycin. Structure 4:1465–1474

Sood S, Malhotra M, Das BK, Kapil A (2008) Enterococcal infections & antimicrobial resistance. Indian J Med Res 128:111–121

Wiederstein M, Sippl MJ (2007) ProSA-web: interactive web service for the recognition of errors in three-dimensional structures of proteins. Nucleic Acid Res 35:W407–W410

Yoon HJ, Lee SJ, Mikami B, Park HJ, Yoo J, Suh SW (2008) Crystal structure of UDP-*N*-acetylglucosamine enolpyruvyl transferase from *Haemophilus influenza* in complex with UDP-*N*-acetylglucosamine and fosfomycin. Proteins 71:1032–1037